

# Calculations of Differential Elastic and Total Reaction Cross Sections of $K^+$ -nucleus Scattering in the Framework of Microscopic Model of Optical Potential

E.V. Zemlyanaya<sup>1</sup>, K.V. Lukyanov<sup>1</sup>, V.K. Lukyanov<sup>2</sup>, K.M. Hanna<sup>3</sup>

<sup>1</sup>e-mail: luky@jinr.ru, elena@jinr.ru, Laboratory of Information Technologies, JINR, Dubna;

<sup>2</sup>Laboratory of Theoretical Physics, JINR, Dubna; <sup>3</sup>Math. and Theor. Phys. Dep., NRC, Atomic Energy Authority, Cairo, Egypt

It is known that the  $K^+$ -meson scattering can be used as a weak hadronic interaction probe for investigating the neutron density distributions in nuclei while the electron scattering is applied to study the nuclear charge density. This is a reason for the special interest to the experimental data on the elastic scattering differential cross sections [1], [2] and also on the total reaction cross sections [3]-[7] of the kaon-nucleus interactions. In one of the first theoretical works [8] the elastic and inelastic differential cross sections of  $K^\pm$ -mesons with momentum 0.8 GeV/c on  $^{12}\text{C}$  and  $^{40}\text{Ca}$  nuclei were calculated using the Glauber high-energy scattering theory [9], and it was calculated that accounting for the multiple scattering terms in the theory does not contribute a noticeable effect to improve the agreement with the experimental data. The Glauber approach has been also applied in Ref. [10] for calculating elastic and inelastic scattering of  $K^+$ -mesons from  $^6,^7\text{Li}$  nuclei where the free  $K^+N$  amplitude and a cluster  $\alpha 2n, \alpha t$  model has been used for these nuclei. In Ref. [11] the optical  $K^+$ -nucleus potential was constructed based on the  $K^+N$  t-matrix and the considered nuclear one particle wave functions were those of a square well potential. The agreement with experimental data was achieved under the addition of 10-15% of  $S_{11}$  phase in the  $K^+N$  amplitude which was motivated as the in-medium effect. Later on in Ref. [12] for the study of  $K^+$  scattering a local version [13] of the Kisslinger potential [14] was applied which has been early suggested for pion-nucleus scattering. In [15] a phenomenological 6-parameter Woods-Saxon optical potential was fitted to the experimental data.

In our study, to avoid introducing the number of phenomenological parameters, we suggest a microscopic optical potential that does not introduce any free parameters and, in contrast, uses the known data both on the target-nucleus structure and the  $K^+N$  scattering amplitude.

## Basic formulas

We use the microscopical optical potential (OP) derived in Ref. [16] on the basis of non-relativistic amplitude at high energy scattering from complex

systems [9], [17], [18] in the so-called optical limit. In fact, the latter approximation means the summation of the  $K^+N$  elementary amplitudes over all the nucleons distributed in the target-nucleus. Both the elementary amplitude and the density distribution function of the bare nucleons are known from experimental data. This model is similar to a folding model but here an elementary  $K^+N$  potential would be used instead of the  $K^+N$  scattering amplitude. Thus, in accordance with [16] we have,

$$U^H = V^H + iW^H = -\frac{\beta_c}{(2\pi)^2} \sum_{\nu=p,n} \sigma_K^\nu (\alpha_K^\nu + i) \times \int_0^\infty dq q^2 j_0(qr) \rho_\nu(q) f_K^\nu(q). \quad (1)$$

Here  $\hbar = c = 1$ ;  $\rho_n(q)$  and  $\rho_p(q)$  are form factors of the bare neutron and proton densities of a nucleus. For  $^{12}\text{C}$  and  $^{40}\text{Ca}$  nuclei we consider them to be of the same form  $\rho_n(q) = \rho_p(q)$ . For  $\rho_p(q)$  we use the symmetrized Fermi function with two parameters cited in [19] where they were reproduced from [20]. As shown in (1) the OP is defined by the total cross section  $\sigma_K^\nu$  for kaon-nucleon interaction and  $\alpha_K^\nu$ , the ratio of real to imaginary part of the  $K^+N$  forward scattering amplitude. In addition, the  $K^+N$  form factor has the form  $f_K^\nu(q) = \exp(-\beta_\nu q^2/2)$ . Values for the quantities  $\sigma_K^\nu$ ,  $\alpha_K^\nu$  and the slope parameter  $\beta_\nu$  were derived in [22] from the known scattering phases for five momenta  $k_{lab}$  from 0.489 to 0.902 GeV/c. For intermediate momenta these parameters were found using the Lagrange approximation method. Thus, the microscopic OP (1) does not have free parameters. It is noticed that in the above considered experimental data, the kinetic energy of the  $K^+$ -meson is comparable to, or larger than its mass, and therefore the problem is to be solved in relativistic frame. To this end, in Eq.(1) for OP one should use the relativistic expression of the kaon c.m. velocity  $\beta_c = k_{lab}/(E + m_1^2/m_2)$ , where  $E = \sqrt{k_{lab}^2 + m_1^2}$  is its total energy in laboratory system. Then, substituting the nuclear potential (1) together with the Coulomb potential  $U_c(r)$  in the Klein-Gordon equation one obtains an equa-

tion of a Shrödinger like form,

$$(\Delta + k^2)\psi(\mathbf{r}) = 2\bar{\mu} \left[ U - \frac{U^2}{2E} \right] \psi(\mathbf{r}) = 2\mu U_{eff}(r)\psi(\mathbf{r}), \quad U_{eff} = \gamma^{(r)} \left[ U - \frac{U^2}{2E} \right], \quad (2)$$

$$U(r) = U^H(r) + U_C(r). \quad (3)$$

Usually in (2) and (3) both the term  $U^2/2E$  and the correction  $m_1^2/m_2E$  for the relativistic velocity  $\beta_c$  can be neglected, and therefore in calculations one uses  $U_{eff} \simeq \gamma^{(r)}U$  and  $\beta_c \simeq \beta = k_{lab}/E$ . In calculations, we take the known expression for the Coulomb potential in the field of the uniform nuclear charge density distribution of radius  $R_C = r_c A^{1/3}$  with  $r_c = 1.3fm$ . In Eq.(2) we take the relativistic  $k$  value in c.m. system as follows,

$$k = \frac{m_2 k_{lab}}{\sqrt{(m_1 + m_2) + 2m_2 T^{lab}}}, \quad (4)$$

where  $T^{lab} = E - m_1$ . In the right hand side of Eq.(2), the quantity  $\bar{\mu} = \mu\gamma^{(r)} = \gamma_1^* m_1 m_2 / (\gamma_1^* m_1 + m_2)$  is the relativistic reduced mass (energy) of the system, from which one follows the non-relativistic reduced mass  $\mu = m_1 m_2 / [m_1 + m_2]$ . In this notation the relativization factor of OP is given by,

$$\gamma^{(r)} = \gamma_1^* \cdot \frac{m_1 + m_2}{\gamma_1^* m_1 + m_2}, \quad (5)$$

where the kaon Lorentz factor in c.m. system is

$$\gamma_1^* = \frac{\gamma_1 m_2 + m_1}{\sqrt{2\gamma_1 m_1 m_2 + m_1^2 + m_2^2}}, \quad \gamma_1 = \frac{E}{m_1}. \quad (6)$$

Equation (2) can be solved using a standard program for solving Shrödinger equation. To this purpose we use code DWUCK4 [23] where one should take the potential  $U_{eff}(r)$ .

It should be noted that there exist a number of expressions for the relativization factors  $\gamma^{(r)}$  obtained, e.g., in [24],[25],[26]. However, our calculations in [27] for the considered energies of the kaon-nucleus scattering show that all the various expressions of  $\gamma^{(r)}$  lead to very close values. As a consequences, for the kaon momenta 0.8 and 0.635 GeV/c in the case of scattering from  $^{12}C$  nucleus these relativization factors get the corresponding values 1.789 ( $\pm 2.5\%$ ) and 1.557 ( $\pm 2\%$ ), while for scattering from  $^{40}Ca$  at 0.8 GeV/c we have  $\gamma^{(r)} = 1.866(\pm 1\%)$ . It was also shown that calculations of the differential cross sections using these different  $\gamma^{(r)}$  do not exceed the experimental bars.

In Fig.1 we show the calculated differential cross sections (solid curves) and the corresponding experimental data. The dashed curves demonstrate

calculations at  $\gamma^{(r)}=1$  which can be conventionally called as the "non-relativistic" case, or better, the "semi-relativistic" one because of the fact, that the momentum  $k$  and velocity  $\beta_c$  in (2) retain their relativistic values. The large difference between solid and dashed curves points to the fact that the relativistic effects are significant. This conclusion is also supported by calculations of total reaction cross sections. Indeed, in the case of the  $K^{(+)}+^{40}Ca$  collision we obtain at  $\gamma^{(r)} = 1$  a value  $\sigma_r^{tot} = 245mb$  but when the relativization is accounted for with  $\gamma^{(r)} = 1.85$  obtained from eq.(5), the corresponding cross section becomes  $367mb^1$ . This indicates that the relativization effect is about 30%.

## Nuclear Structure Effect

As already noticed, the calculated microscopic OPs depend on the distribution function of point like neutrons and protons in the ground state of a nucleus. These functions can be derived both from nuclear model calculations and defined from independent experimental data. We applied three forms of the  $^{12}C$  density  $\rho(r)$  for distributions of the point-like nucleons. Parameters of the Fermi type density distribution

$$\rho(r) = \rho_0 \left[ 1 + \exp \frac{r-c}{a} \right]^{-1} \quad (7)$$

were estimated in [29] basing on the shell model calculations. This form was applied in many works for calculations of the nucleus-nucleus folding potentials. Two other densities are taken from Refs. [19]-[21] and from [30]. In Refs. [19]-[20], for the  $^{12}C$  density  $\rho(r)$ , the symmetrized two-parameter Fermi function was used being close to that given in Eq.(7), while in [30], the 3-parameter form of Fermi function was used for the same density,

$$\rho(r) = \rho_0 \left[ 1 + \omega \frac{r^2}{c^2} \right] \times \left[ 1 + \exp \frac{r-c}{a} \right]^{-1}. \quad (8)$$

Fig. 2 shows the tested densities  $\rho(r)$  of the  $^{12}C$  nucleus and the corresponding differential cross sections of the  $K^+$ -meson scattering at different momenta. It is seen that some difference in the calculated cross sections can be noticed in the range of large angles of scattering but it is difficult to distinguish between the different curves. With respect to the total cross sections  $\sigma_r^{tot}$  they differ from each others by less than 1%. This is too small a quantity to hope to get better agreement with the total cross sections by improving the one-particle model calculations of the ground state nuclear density distributions.

<sup>1</sup>As to the experimental value for this cross section, the data from [3]-[7] on the  $K^+ + ^{40}Ca$  reaction at 0.714 GeV/c were reconsidered in [28] yielding  $412.9 \pm 5.5mb$ .

## Total Cross Sections

The suggested microscopical model of the  $K^+A$  optical potential and the relativization of the problem enable one to explain successfully the  $K^+A$  differential cross section without any free parameters. As to the total cross sections, the problem to get close agreement with the experimental data is still open. It was shown that without relativization the calculated total cross sections were lower by about 30% in comparison with the experimental data, while with inclusion of relativization the disagreement with the data is reduced to about 10-15%. However, further attempts to improve the result by including quadratic  $U^2/2E$  terms in the potential and by using other forms of the density distribution function of the target nucleus do not result in the desired correction. It is worthy of note that this problem related to the total cross sections has a long history. A lot of different mechanisms have been suggested to account for the so-called in-medium corrections for the kaon interaction with the nuclei. In our study we want to draw attention to another purely nuclear mechanism for the interpretation of the mentioned discrepancy. We suggest to take into consideration the effects connected with excitations of the nuclear collective states as well as the channels inherent in the nucleon removal reactions. It is well known that these processes play an important role in the nucleon- and nucleus-nucleus collisions and their effect on the elastic scattering can be as usually taken into account by introducing an additional imaginary potential in the peripheral region of the basic OP. To test the role of this mechanism, we modified the optical potential given in Eq. (3) to

$$U(r) \implies U(r) - gr \frac{d(\text{Im}U)}{dr}, \quad (9)$$

i.e., by adding the derivative of the imaginary part of our microscopic OP. This term has a "bump" in the periphery zone and its strength is defined by the selection of the free parameter  $g$ . In Fig. 3 it is shown the effect of surface absorption on the differential cross sections of elastic scattering of  $K^+ + {}^{12}\text{C}$  at momenta 0.635 and 0.715 GeV/c. At the same momenta there exist the data on total reaction cross sections presented in Ref. [28]. These are  $\sigma_r^{\text{tot}}(0.656/, \text{GeV}/c) = 141.8 \pm 1.5$  mb and  $\sigma_r^{\text{tot}}(0.714/, \text{GeV}/c) = 149.3 \pm 1.5$  mb. From Fig. 3 it is obvious that the addition of the surface absorption potential with  $g = 0.07$  and  $g = 0.1$  at momenta 0.635 and 0.715 GeV/c respectively, give little change in the differential cross sections values. At the same time, such an addition leads to the growth of the total cross sections from 125 mb to 140 mb at momentum 0.635 GeV/c and from

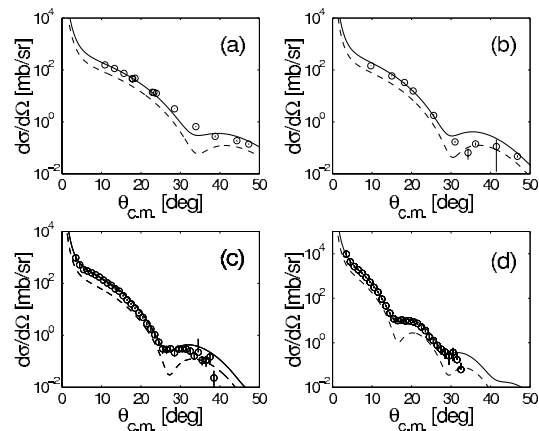


Figure 1: Differential cross sections for  $K^+$ -nucleus scattering. For target-nucleus  ${}^{12}\text{C}$ : (a) – at 0.635 GeV/c, (b) – at 0.715 GeV/c, (c) – at 0.8 GeV/c; (d) – for target-nucleus  ${}^{40}\text{Ca}$  at 0.8 GeV/c. Solid curves – with the relativization included, dashed – "non-relativistic" calculations. Experimental data from [1,2].

129 mb to 149 mb at momentum 0.715 GeV/c which result in a good agreement with the given above experimental data. Thus, there arrives a possibility to describe simultaneously both the data of the total reaction and differential elastic scattering cross sections based on the elementary  $K^+N$  interaction and by accounting for the nuclear dynamics of the scattering process. In this case, the microscopic theory should be developed so that to take into account not only for the single-particle mechanism of the reaction but also effects of the inter-nucleus correlations, collective excitations, and coupling with the nuclear reaction channel in continuum, the factors which may affect the value of the parameter  $g$ .

## Conclusions

We conclude that for explanation of the behavior of angular distributions of the  $K^+$ -mesons scattering on nuclei, it suffices to use a simple model optical potential given by Eq.(1) without using any free parameters. In this model the energy dependence is included in the elementary  $K^+N$  scattering amplitude which is known from different independent experimental data. In that respect it is not necessary to make the model more complicated by introducing, e.g., the non-local terms in OP as they occur in the Kisslinger model or using a phenomenological optical potential with a large number of free parameters. We notice that, when analyzing the experimental data, the relativistic effects were found to play an important role. Thus, it was not possible to describe the angular distributions of the elastic

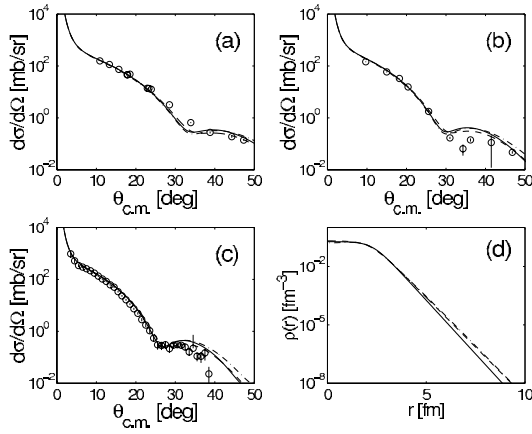


Figure 2: Elastic scattering of  $K^+$ -mesons on  $^{12}\text{C}$  calculated at different density distributions, (a) – at 0.635 GeV/c, (b) – at 0.715 GeV/c, (c) – at 0.8 GeV/c, (d)– density distribution functions. Solid curves – for densities from [19,20], dash-dotted – from [29], dashed – from [30]. Experimental data from [1,2].

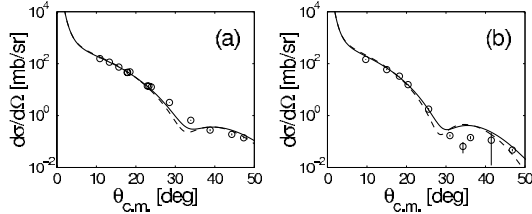


Figure 3: Elastic scattering of  $K^+$ -mesons on  $^{12}\text{C}$ : (a) – at 0.635 GeV/c and (b) – at 0.715 GeV/c. Solid curve – without "surface" term in OP, dashed – with "surface" term eq.(12): (a) – at  $g=0.07$ ; (b) – at  $g=0.1$ . Experimental data from [2].

scattering of kaons on nuclei and also to exclude the strong discrepancy between the calculated and the experimental data of total cross sections without relativization. One can also note that the small difference between nuclear one-particle density distributions predicted by different models weakly affects the calculated results of both the elastic and total cross sections. The same can be said on the role of  $U^2/2E$  terms in optical potential which appear when transforming the Klein-Gordon equation to the relativistic Schrödinger one. In this connection, to interpret the data of the total cross sections it was suggested the nuclear mechanism for the additional absorption in the peripheral region of the elastic channel by introducing an imaginary potential to the basic OP. This phenomenological potential permits to account for an effect on the elastic channel of the virtual channels of both excitations of nuclear collective states and of direct

nucleon removal reactions available at energies of incident kaons.

## References

- [1] D. Marlow et al., Phys. Rev. **C 25**, 2619 (1982).
- [2] R.E. Chrien et al., Nucl. Phys. **A 625**, 251 (1997).
- [3] D. Bugg et al., Phys. Rev. **168**, 1466 (1968).
- [4] Y. Mardor et al., Phys. Rev. Lett., **65**, 2110 (1990).
- [5] R.A. Krauss et al., Phys. Rev. **C 46**, 655 (1992).
- [6] R. Sawafta et al., Phys. Lett. **B 307**, 293 (1993).
- [7] R. Weiss et al., Phys. Rev. **C 49**, 2569 (1994).
- [8] Y. Abgrall and J. Labarsouque, Nucl. Phys. **A 426**, 431 (1984).
- [9] R.J. Glauber, Lectures in Theoretical Physics. N.Y.: Interscience, 1959. P.315.
- [10] M.A. Zhusupov, E.T. Ibraeva, Yad. Fiz. **64**, 2003 (2001).
- [11] P.B. Siegel, W.B. Kaufmann, W.R. Gibbs, Phys. Rev. **C 30**, 1256 (1984).
- [12] A.A. Ebrahim and S .A.E. Khallaf, Phys. Rev. **C 66**, 044614 (2002).
- [13] M.B. Jonhson and G.R. Satchler, Ann.Phys. (N.Y.) **248**, 134 (1996).
- [14] L.S. Kisslinger, Phys. Rev. **98**, 761 (1955).
- [15] A.A. Ebrahim and S.A.E. Khallaf, J. Phys. **G 30**, 83 (2004).
- [16] V.K. Lukyanov, E.V. Zemlyanaya, K.V. Lukyanov, Phys. At. Nucl. **69**, 240 (2006), (transl. from Yad.Fiz. **69**, 262 (2006)).
- [17] A.G. Sitenko, Ukrainian Fiz. J., **4**, 152 (1959).
- [18] W. Czyz and L.C. Maximon, Ann. of Phys. **52**, 59 (1969).
- [19] V.K. Lukyanov, E.V. Zemlyanaya, B. Słowiński, Phys. At. Nucl. **67**, 1282 (2004), (transl. from Yad.Fiz. **67**, 1306 (2004)).
- [20] V.V. Burov, V.K. Lukyanov, Preprint 4-11098, JINR (Dubna, 1977).
- [21] V.V. Burov, D.N. Kadrev, V.K. Lukyanov, Yu.S. Pol', Phys. At. Nucl. **61**, 525 (1998), (transl. from Yad.Fiz. **61**, 595 (1998)).
- [22] K. Yamaguchi K., Y. Sakamoto, Nuovo Cim. **A 108**, 893 (1995).
- [23] P.D. Kunz P.D., E. Rost, Computational Nuclear Physics Vol.2 (Eds: Langanke K. et al.) Springer Verlag, 1993. P.88.
- [24] A. Ingemarsson, Phys. Scripta **9**, 156 (1974).
- [25] G. Fäldt, A. Ingemarsson, J. Mahalanabis, Phys. Rev. **C 46**, 1974 (1992).
- [26] M.L. Goldberger, K.M. Watson, Collision Theory,(John Willey & Sons,INC., New York-London-Sidney), 1964.
- [27] V.K. Lukyanov, E.V. Zemlyanaya, K.V. Lukyanov, and K.M. Hanna, arxiv:0812.4598 (2009).
- [28] E. Friedman e.a., Phys.Rev., **C 55**, 1304 (1997).
- [29] M. El-Azab Farid and G.R. Satchler, Nucl. Phys. **A 438**, 525 (1985).
- [30] J.D. Patterson, R.J. Peterson, Nucl. Phys. **A 717**, 235 (2003).